GEOPHYSICAL RESEARCH LETTERS, VOL. 27, NO. 17, PAGES 2797-2800, SEPTEMBER 1, 2000

Solar cycle effects in planetary geomagnetic activity: Analysis of 36-year long OMNI dataset

V. O. Papitashvili[1]

Space Physics Research Laboratory, University of Michigan, Ann Arbor, Michigan

N. E. Papitashvili[2] and J. H. King

National Space Science Data Center, NASA/Goddard Space Flight Center, Greenbelt, Maryland

Abstract. NSSDC's OMNI dataset, which now spans 1963–1999, contains a collection of hourly means of interplanetary magnetic field (IMF) and solar wind (SW) plasma parameters measured near the Earth's orbit, as well as some auxiliary data. We report a study of solar cycle effects in planetary geomagnetic activity in which 27-day averages of several OMNI parameters are compared with equivalent *Kp* and *Dst* averages. Some established trends in these parameters over solar cycles are confirmed; for example, it is concluded that changes in the magnitude (rather than in direction) constitute the primary solar cycle variation in the IMF. However, this study also reveals that long-term changes in planetary geomagnetic activity are driven more actively by solar wind–magnetosphere coupling of an electrodynamic nature rather than by plasma transport into the magnetosphere. This suggests that ambient (background) interplanetary "electric" environment (in which the Earth's magnetosphere is immersed over the solar cycles) may play a more significant role in causing changes in the frequency of geomagnetic storms and substorms than previously realized.

1. Introduction

Since the discovery of the solar wind, numerous studies have been undertaken to investigate its variability with the solar cycle [e.g., *Gazis,* 1996]. Though a number of studies have dealt with long-term correlations between solar wind and geomagnetic activity [e.g., *Crooker and Gringauz,* 1993; *Gonzalez et al.,* 1993; *Kamide et al.,* 1998, *Stamper et al.,* 1999, and references therein], the character and dynamics of the solar wind interaction with the geomagnetic field on a scale of decades have been studied very little [e.g., *Papitashvili,* 1982; *Petrinec et al.*, 1991].

The 36-year long, IMF/SW multi-source OMNI dataset is maintained at the National Space Science Data Center, NSSDC [*King and Papitashvili*, 1994; http://nssdc.gsfc.nasa.gov/omniweb]. Over its history, the dataset has been utilized in numerous studies, mainly by using hourly means. Recently daily and 27-day averages were made available; these new options provide an excellent opportunity for studies of either IMF polarity or seasonal effects from daily data or solar cycle effects from 27-day averages where the IMF polarity effect is greatly reduced. In addition to the IMF/SW parameters, the OMNI dataset contains some auxiliary data including sunspot numbers and geomagnetic indices. In this study, we focused on solar cycle effects in the planetary geomagnetic activity indices *Kp* and *Dst.*

2. Data

Figure 1 (left) shows time series of sunspot numbers R (bottom) together with the IMF magnitude B_T, components B_x, B_y, B_z (in GSM coordinates), solar wind speed, and plasma density and temperature from November 1963 through November 1999. OMNI's hourly data were averaged up to daily averages that were then further averaged over the 27-day intervals defining Bartels rotation numbers. Though the suggested averaging interval is approximately a month long, it might better reflect the physics of the solar wind escape (away from the Sun) during successive solar rotations. That averaging also helps to suppress effects of IMF polarity, allowing us to study solar-cycle-long variations using relatively high time resolution data. All the results presented below were obtained by utilizing 27-day averages made separately for each of the IMF/SW parameters; additional time series (shown on the right) are constructed from these averages. *Stamper et al.* [1999] have recently shown that averages made, for example, as $\langle N_{SW}\rangle\langle V_{SW}\rangle^2$ and $\langle N_{SW} V_{SW}^2\rangle$, are very similar.

Visual inspection clearly reveals that B_T varies clearly with a period of ~11-years through solar activity cycles 21 and 22 and that its maxima overlap with the descending phase of the solar cycle [e.g., *King,* 1991]. B_T increases again with the ascending phase of the 23rd cycle. However, the field magnitude was almost flat (varied within ±1 nT) during the entire 20th solar cycle. The latter is confirmed by insignificant cycle-20 variation of B_x and B_y components. An interesting feature of the B_x and B_y variations is that they show "pearls" of ~1-year pulsations reaching magnitude ±2 nT (especially B_x). The "pearls" are mainly seen during the ascending phases of the 20th and 21st solar cycles and then through the solar minimum and over the ascending phase of the 23rd cycle. It is obvious that these "pearls" appear because the Earth (in its orbit around the Sun) spends some time above or below the heliospheric current sheet (HSC). The pearls are less evident near solar maxima mainly because the HCS is sufficiently distorted and/or structured so that the fraction of "positive" *vs.* "negative" IMF polarity which the Earth experiences during its annual excursion about the Sun is only weakly related to the heliolatitude of the Earth. That the pearls are somewhat clearer in B_x than in B_y suggests that the IMF may be pulled radially outward more than the Parker spiral.

[1]Also at Danish Meteorological Institute, Copenhagen, Denmark
[2]Also at Raytheon ITSS, NASA/GSFC, Greenbelt, Maryland

Paper number 2000GL000064.
0094-8276/00/2000GL000064$05.00

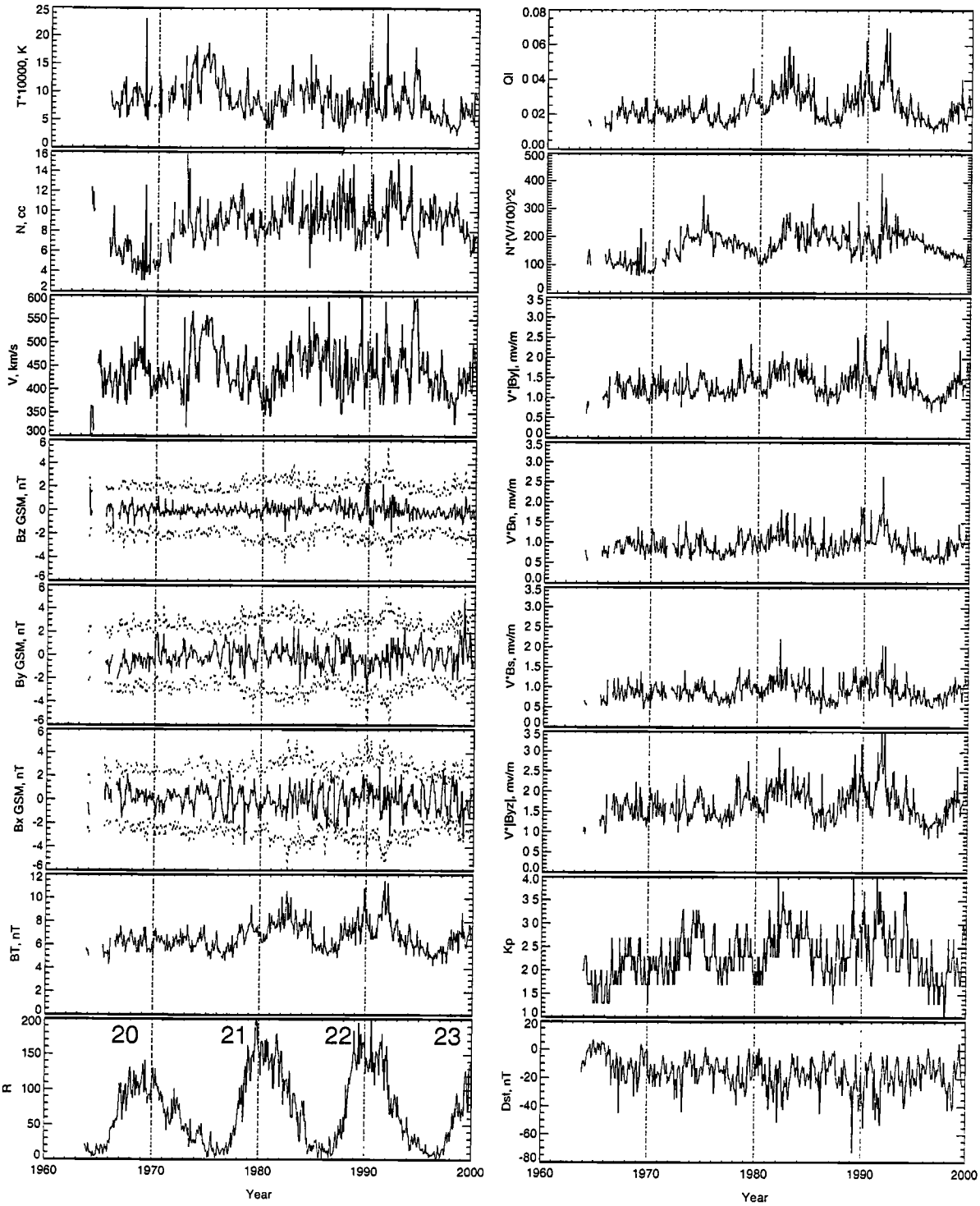

Figure 1. 27-day averages of some OMNI parameters from November 1963 through November 1999 in comparison with geomagnetic activity indices *Kp* and *Dst*, solar wind dynamic pressure, and various components of the interplanetary electric field. The solar cycle numbers (20, 21, 22, and 23) are printed at the bottom plot on the left panel.

The IMF B_z graph (solid curve in the middle of the corresponding panel) is generally featureless during all 36 years; it varies mainly within ±1 nT. However, it is known that B_z imposes a "half-wave rectifier" effect on the Earth's magnetosphere; therefore, we might expect that only periods (within 27 days) with $B_z < 0$ are geoeffective. The top and bottom (dotted) graphs on the same panel show the 27-day averages of $B_n = B_z > 0$ and $B_s = B_z < 0$, respectively; that is, only positive (negative) hourly B_z values contribute to the 27-day B_n (B_s) averages. These graphs show clearly that both components (~2 nT in average) have similar solar cycle variations and these are similar to the variations of B_T.

We also plotted as the top and bottom dotted graphs (in the same panels where we discussed "pearls") the 27-day averages of positive and negative B_x and B_y, respectively, made in the same manner as B_n and B_s. As seen, these components (~3 nT in average) show similar solar cycle variations as the IMF B_n and B_s and they are again in concert with variations in B_T.

This allows us to draw the conclusion that changes in the magnitude (rather than in direction) constitute the primary solar cycle variation in the IMF.

The solar wind velocity shows weak ~11-year variations around ~450 km/s; they reach maximum values (500–550 km/s) prior to (or almost at) the solar cycle minima, in agreement with findings by *Tsurutani et al.* [1995]. This periodicity is mainly seen during solar activity cycles 21 and 22; the solar wind speed for the outermost cycles (20^{th} and beginning of 23^{rd}) shows less pronounced regularity. Similar weak solar cycle variations are also seen in the temperature graph (top panel). However, solar cycle effects are not pronounced in the SW density time series (note that in building OMNI, pre-1971 density values could not be cross-normalized to post-1971 values due to paucity of overlapping data points in 1971).

There are dual peaks in the sunspot numbers occurring near solar maxima; this feature is also clearly seen as depressions in the IMF B_T variations in years 1969, 1980, and 1991. Similar depressions in the solar cycle variation are seen during the same years in the solar wind velocity but not in the time series of density or temperature. We note that *Kp* and *Dst* indices show a decrease in geomagnetic activity during these years [e.g., *Gonzalez et al.*, 1993].

Osherovich et al. [1999] recently introduced a new index of solar activity defined as the solar wind quasi-invariant (energy density ratio) $QI = (B_T^2/8\pi)/(N \cdot V^2/2)$. They have shown that this index highly correlates with the sunspot numbers *R* (up to $r = 0.98$); therefore, we decided to calculate and to also plot this index to see its solar cycle variation (Figure 1, top right plot). As expected, the *QI* graph mainly resembles variations in the IMF B_T.

3. Analysis

The two bottom panels on the right of Figure 1 show geomagnetic activity indices *Dst* and *Kp*. Visual inspection and comparisons of these indices with the IMF/SW parameters reveal that the long-term variation in 27-day averages of the *Kp* index mainly follows the corresponding variations in B_T and somewhat in dynamic pressure $p \sim N \cdot V^2$, however, the corresponding changes of the lower-bounding envelop of *Dst* does not follow similar variations in *Kp* or any of other solar wind parameters.

To further investigate these results we produced a number of derivatives from the IMF/SW 27-day averages such as the "merging" interplanetary electric field (IEF) $E_T = V_{SW} \cdot |B_{yz}|$ and its components: the "dawn-dusk" $E_{dwds} = V_{SW} \cdot B_s$, "dusk-dawn" $E_{dsdw} = V_{SW} \cdot B_n$, and "north-south" $E_{ns} = V_{SW} \cdot |B_y|$ electric fields. Here $|B_{yz}| = (\langle B_y \rangle^2 + \langle B_z \rangle^2)^{1/2}$ is the total IMF "clock-angle" vector calculated from the corresponding 27-day averages and taken in the Y–Z GSM plane, transverse to the SW velocity direction.

One can clearly see in Figure 1 that E_T and its components are all in concert (i.e., visually correlate very well) with *Kp*, but not with the *Dst* index. Moreover, the dusk-dawn component E_{dsdw} (controlled by IMF B_n) highly agrees with the "half-wave rectifier" component E_{dwds} (controlled by IMF B_s). Both electric field components show similar level of correlation with *Kp* reflecting the fact that, at 27-day resolution, the IMF northward and southward components vary in phase (except for sign) over three solar cycles. The IMF near-ecliptic components show similar behavior when averaged only for a certain sign (dotted graphs in a middle of the left panel).

The IEF E_{dwds} and E_{dsdw} components are of the same magnitude and their lowest values are near 0.5 mV/m. At the same time, the lowest values of E_{ns} (controlled by IMF B_y) are ~1 mV/m, comparable with the corresponding lowest values of E_T, but twice as much as the lowest values of E_{dwds}. As a result of IMF B_y being on average larger than B_z, the most significant contribution to the magnitude of E_T comes from E_{ns} rather than from the "half-wave rectifier" component E_{dwds} to which the commonly adopted view delegates the more active role in geomagnetic activity.

Table 1. Correlation Coefficients Between the IMF/SW 27-Day Averaged Parameters, Their Derivatives, and *Kp* and *Dst* Indices

27-day averages	*Kp*	*Dst*
IMF B_T	0.61	0.54
IMF B_x	0.14	0.09
IMF $B_x < 0$	0.56	0.45
IMF $B_x > 0$	0.61	0.46
IMF B_y	0.10	0.02
IMF $B_y < 0$	0.36	0.33
IMF $B_y > 0$	0.28	0.33
IMF B_z	0.15	0.20
IMF $B_z < 0$	0.43	0.53
IMF $B_z > 0$	0.31	0.37
SW velocity, *V*	0.70	0.40
SW temperature, *T*	0.63	0.30
SW density, *N*	0.03	0.06
$E_{IMF} = V \cdot B_T$	0.82	0.62
$E_T = V \cdot \lvert B_{yz} \rvert$	0.70	0.61
$E_{dawn\text{-}dusk} = V \cdot B_s$	0.69	0.66
$E_{dusk\text{-}dawn} = V \cdot B_n$	0.58	0.51
$E_{north\text{-}south} = V \cdot \lvert B_y \rvert$	0.61	0.51
$p \sim N \cdot V^2$	0.60	0.38
$QI \sim B_T^2 / N \cdot V^2$	0.60	0.53

To verify our observations, we cross-correlated all IMF/SW parameters plotted in Figure 1 with the *Kp* and *Dst* indices. Table 1 lists resultant correlation coefficients. The first and least expected result is the higher correlation between the "toward/away" IMF B_x components and geomagnetic activity indices in comparison with IMF B_n and B_s; this effectively brings the IMF B_x component into the play in controlling global geomagnetic activity. Normally the geoeffectiveness of B_x is assumed to be negligible [e.g., *Gonzales and Mozer*, 1974], however, our results imply some unappreciated geoeffectiveness of B_x, possibly associated with high latitude reconnection between the IMF and the magnetospheric lobe field lines indirectly affecting global geomagnetic activity.

One can see that E_{dwds}, E_T, and V_{SW} are the parameters that mostly affect planetary geomagnetic activity as described by the *Kp* index ($r = 0.69$, 0.70, and 0.70, respectively). However, the most geoeffective IMF/SW parameter is $E_{IMF} = V_{SW} \cdot B_T$ showing the highest correlation with *Kp* ($r = 0.82$). The latter may be considered as a combination of effects of E_T and B_x. The next group of parameters B_T, $B_x > 0$, $B_x < 0$, SW temperature, dynamic pressure, and *QI* index correlate with *Kp* at the level $r \sim 0.6$; it is surprising that the "half-wave rectifier" component $B_z < 0$ shows even weaker correlation ($r = 0.43$), comparable with its counterpart component $B_z > 0$ ($r = 0.31$).

As shown by *Burton et al.* [1975], *Dst* should better correlate with the IEF E_{dwds} component (r = 0.66) than with any other IMF/SW parameter. Most of the other parameters B_T, $B_z < 0$, E_{dsdw}, E_{ns}, and *QI* show correlation with *Dst* at the level $r \sim 0.5$. The solar wind speed and dynamic pressure correlate with *Dst* at the level of $r \sim 0.4$. On the other hand, one can expect that 27-day intervals that contain major magnetic storms should show a clear correlation with large values of either the IMF B_s or the solar wind dynamic pressure. Close inspection of Figure 1 reveals that even "spike-like" changes in the dynamic pressure have almost nothing in common with changes in the *Dst* index. Thus, over the long-term time scale *Dst* shows a weaker correlation in general with most of listed IMF parameters than does *Kp*.

We correlated 27-day averages of B_T with similar averages of all components B_x, B_y, and B_z (central solid curves on the corresponding panels) to see whether any components could be the major driver behind of the total value. However, the obtained cross-correlation coefficients are ~0.05 for all components. While this result confirms that changes in the IMF strength and direction are statistically uncorrelated [e.g., *Papitashvili and Gromova*, 1982], one can expect that any of $|B_x|$, $|B_y|$, $|B_z|$, $(B_x^2 + B_y^2)^{1/2}$, or $(B_y^2 + B_z^2)^{1/2}$ should highly correlate with B_T reaching $r \sim 0.8$.

Plotting 27-day averages of the IMF "toward/away" B_x and B_y and "north/south" B_z components separately (dotted graphs in Figure 1), we revealed that their 36-year long time series over 3.5 solar cycles change very much in concert with the IMF B_T. That gives no preference to any of these components to be larger (or smaller) than another component during different phases of the solar cycle; therefore, their cumulative effect on global geomagnetic activity is sufficiently described by B_T over long-term time scales.

Also, to check the impact of using 27-day averages we ran correlations of *Kp* and *Dst* indices with many of the above-mentioned IMF/SW parameters using daily means for the entire 36-year intervals and then using 3-hour averages over threes years near solar maximum (1979–1981). In the latter case, we first correlated the variables taken for the current 3-hour interval, and then we took the IMF/SW parameters for the previous 3-hour interval. However, the obtained correlation coefficients are ~20% smaller in comparison with numbers given in Table 1. This may indicate that physics of the solar wind–magnetosphere interaction is manifested in different ways at various time scales; however, investigation of these differences is out of scope of this study.

4. Conclusions

In this study, we focused on the solar cycle effects in the *Kp* index that represents global geomagnetic activity, and in the *Dst* index that measures the ring current development caused by the magnetic storms and (possibly) by some major substorms. Noting that reconnection transfers flux from the dayside (subsolar magnetosphere) to the nightside (magnetospheric tail) and that the solar wind "quasi-viscous" interaction with the magnetosphere drags geomagnetic field lines toward the tail as well, one can expect that the IMF B_s and solar wind velocity (the IEF dawn-dusk component) should be the major drivers for planetary geomagnetic activity.

However, this study reveals that over the long time scale the "total interplanetary electric field" $E_{IMF} = V_{SW} \cdot B_T$ (in which the Earth's magnetosphere is immersed) plays the most significant role in driving global geomagnetic activity represented on the planetary scale by the *Kp* index (r = 0.82). For example, if the IMF B_x were removed from B_T, then the correlation (between E_T and *Kp*) drops to 0.70 showing the unappreciated importance of the IMF B_x-component as noted earlier. Taking into account that both the "toward" and "away" components of B_x show unexpectedly high correlation with *Kp*, we speculate that the highest geoeffectiveness of E_{IMF} means that the combined effect of variations in E_T and B_x keeps global geomagnetic activity continuously "on the boil". Though it seems that the IMF B_x does not contribute directly to the near-Earth interplanetary electric field components, we speculate that ambient (background) interplanetary "electric" environment (in which the Earth's magnetosphere is immersed over the solar cycles) may play a more significant role in causing changes in the frequency of geomagnetic storms and substorms than previously realized.

Acknowledgments. This work was supported from the NSF awards ATM-9628706 and ATM-9727554 to the University of Michigan, as well as partially from the Ørsted satellite project funded by the Danish Government.

References

Burton, R. K., R. L. McPherron, and C. T. Russell, An empirical relationship between interplanetary conditions and *Dst*, *J. Geophys. Res., 80*, 4204, 1975.

Crooker, N. U., and K. I. Gringauz, On the low correlation between long-term averages of solar wind speed and geomagnetic activity after 1976, *J. Geophys. Res., 98*, 59, 1993.

Gazis, P. R., Solar cycle variation in the heliosphere, *Rev. Geophys., 34*, 379, 1996.

Gonzalez, A. L. C., W. D. Gonzalez, and S. L. G. Dutra, Periodic variation in the geomagnetic activity: A study based on the Ap index, *J. Geophys. Res., 98*, 9215, 1993.

Gonzalez, W. D., and F. S. Mozer, A quantitative model for the potential resulting from reconnection with an arbitrary interplanetary magnetic field, *J. Geophys. Res., 79*, 4186, 1974.

Kamide, Y. et al., Current understanding of magnetic storms: Storm–substorm relationships, *J. Geophys. Res., 103*, 17,705, 1998.

King, J. H., Long-term solar wind variations and associated data sources, *J. Geomag. Geoelectr., 43*, Suppl., 865, 1991.

King, J. H., and N. E. Papitashvili, *Interplanetary Medium Data Book, Supplement 5, 1988–1993*, NSSDC/WDC-A-R&S 94-08, NASA/National Space Science Data Center, GSFC, Greenbelt, Maryland, 1994.

Osherovich, V. A., J. Fainberg, and R. G. Stone, Solar wind quasi-invariant as a new index of solar activity, *Geophys. Res. Lett., 26*, 2597, 1999.

Papitashvili, V. O., Relationship between geomagnetic variations in the polar cap and the interplanetary magnetic field during the solar activity cycle, *Geomagn. Aeron., 22, Engl. Transl.*, 130, 1982.

Papitashvili, V. O., and L. I. Gromova, Correlation relations between components of the interplanetary magnetic field and the solar wind velocity, *Geomagn. Aeron., 22, Engl. Transl.*, 99, 1982.

Petrinec, S. P., P. Song, and C. T. Russell, Solar cycle variations in the size and shape of the magnetopause, *J. Geophys. Res., 96*, 7893, 1991.

Stamper, R., M. Lockwood, M. N. Wild, and T. D. G. Clark, Solar causes of the long-term increase in geomagnetic activity, *J. Geophys. Res., 104*, 28,325, 1999.

Tsurutani, B. T., W. D. Gonzalez, A. L. C. Gonzalez, F. Tang, J. K. Arballo, and M. Okada, Interplanetary origin of geomagnetic activity in the declining phase of the solar cycle, *J. Geophys. Res., 100*, 21,717, 1995.

J. H. King and N. E. Papitashvili NSSDC, Code 633, NASA Goddard Space Flight Center, Greenbelt, MD, 20771 (e-mail: king@nssdca.gsfc.nasa.gov, natasha@nssdca.gsfc.nasa.gov)

V. O. Papitashvili, SPRL, University of Michigan, 2455 Hayward St., Ann Arbor, MI, 48109-2143 (e-mail: papita@umich.edu)

(Received March 16, 2000; revised June 7, 2000;
accepted June 30, 2000.)